



저작자표시-비영리-변경금지 2.0 대한민국

이용자는 아래의 조건을 따르는 경우에 한하여 자유롭게

- 이 저작물을 복제, 배포, 전송, 전시, 공연 및 방송할 수 있습니다.

다음과 같은 조건을 따라야 합니다:



저작자표시. 귀하는 원저작자를 표시하여야 합니다.



비영리. 귀하는 이 저작물을 영리 목적으로 이용할 수 없습니다.



변경금지. 귀하는 이 저작물을 개작, 변형 또는 가공할 수 없습니다.

- 귀하는, 이 저작물의 재이용이나 배포의 경우, 이 저작물에 적용된 이용허락조건을 명확하게 나타내어야 합니다.
- 저작권자로부터 별도의 허가를 받으면 이러한 조건들은 적용되지 않습니다.

저작권법에 따른 이용자의 권리는 위의 내용에 의하여 영향을 받지 않습니다.

이것은 [이용허락규약\(Legal Code\)](#)을 이해하기 쉽게 요약한 것입니다.

[Disclaimer](#)

**Master's Thesis**

**Retinex-Based Low Contrast Image Enhancement  
Using Adaptive Tone-Mapping**

Hyo-Gi Lee

Electrical Engineering Program  
Graduate School of UNIST

2016

# **Retinex-Based Low Contrast Image Enhancement Using Adaptive Tone-Mapping**

Hyo-Gi Lee

Electrical Engineering Program  
Graduate School of UNIST

# **Retinex-Based Low Contrast Image Enhancement Using Adaptive Tone-Mapping**

A thesis

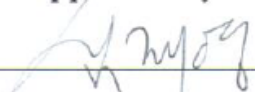
Submitted to the Graduate School of UNIST

in partial fulfillment of the  
requirements for the degree of  
Master of Science

Hyo-Gi Lee

12. 10. 2015

Approved by



Major Advisor

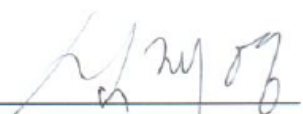
Jae-Young Sim


# **Retinex-Based Low Contrast Image Enhancement Using Adaptive Tone-Mapping**

Hyo-Gi Lee

This certifies that the thesis of Hyo-Gi Lee is approved.

12. 10. 2015

  
\_\_\_\_\_  
Advisor: Jae-Young Sim

  
\_\_\_\_\_  
Seung-Joon Yang: Thesis Committee Member #1

  
\_\_\_\_\_  
Se-Young Chun: Thesis Committee Member #2

## Abstract

In this paper, we enhance low contrast images using the human visual system based Retinex theory and adaptive tone-mapping. We try to reduce halo artifact and color inconsistency, but also preserve naturalness of images. In the proposed algorithm, we process only the Y channel of the Yuv color space rather than RGB color space to maintain color-constancy. We first apply an adaptive bilateral filtering on the Y channel image to alleviate halo artifact during enhancement. Then we partition the intensity range of probability distribution of filtered Y channel image into low, middle, and high contrast regions according to a cost function. We improve the contrast of filtered Y channel image by using A-law based tone mapping by stretching the low contrast regions and compressing the high contrast regions adaptively. Experimental results show that the proposed algorithm enhances the visibility of input low contrast images efficiently.



## Contents

<b>I. Introduction</b> .....	<b>1</b>
<b>II. Previous Works</b> .....	<b>4</b>
2.1 Retinex based on RGB Color Space .....	<b>4</b>
2.2 Retinex based on Light Channel .....	<b>7</b>
<b>III. Proposed Algorithm</b> .....	<b>9</b>
3.1 Overview .....	<b>9</b>
3.2 Adaptive Bilateral Filtering .....	<b>9</b>
3.3 Contrast Region Partitioning .....	<b>12</b>
3.3.1 Global Estimation .....	<b>13</b>
3.3.2 Local Estimation .....	<b>14</b>
3.3.3 Exception Processing .....	<b>15</b>
3.4 Adaptive A-law Based Tone Mapping .....	<b>15</b>
3.4.1 A-law Based Tone Mapping .....	<b>16</b>
3.4.2 Weighted A-law Based Tone Mapping .....	<b>18</b>
3.5 Final Enhanced Image .....	<b>19</b>
<b>IV. Experimental Results</b> .....	<b>20</b>
<b>V. Conclusion</b> .....	<b>33</b>
<b>References</b> .....	<b>34</b>



## List of Figures

Figure 1.1	Low contrast image enhancement. (a) An input low contrast image and (b) the enhanced image. Probability distributions of (c) input Y channel and (d) the enhanced Y channel. ....	2
Figure 2.1	Retinex-based image enhancement. (a) An input low contrast image and (b) the enhanced image by using SSR. The enlarged images of the blue rectangles in (c) the input image and (d) the enhanced image. (e) The enlarged image of the red rectangle in the enhanced image. ....	5
Figure 2.2	Comparison of image enhancement results: (a) MSR and (b) MSRCR.	6
Figure 2.3	Light channel based Retinex algorithms. The flow charts of (a) [9] and (b) [8] and [9]. The enhanced images by using (c) [9] and (d) [8] and [9]. ....	7
Figure 3.1	Flowchart of the proposed algorithm. ....	9
Figure 3.2	Neighboring pixels in ABF. (a) Neighboring set $P(x, y)$ of $(x, y)$ in bilateral filtering. (b) Neighboring set $S(x, y)$ of $(x, y)$ in ABF.	11
Figure 3.3	Results of ABF. (a) Original image. (b) Bilateral filtering result. (c) Guided filtering result. (d) ABF result. (e), (f), and (g) are the enlarged images of (b), (c), and (d), respectively. ....	12
Figure 3.4	Global estimation for low contrast region. (a) Initial contrast region labeling. (b) Merged contrast region labeling. ....	13
Figure 3.5	Local estimation for low-contrast region. (a) Process of local estimation. (b) Result of local estimation labeling. ....	14
Figure 3.6	Exception handling of contrast region labeling. (a) Local contrast region labeling. (b) Final estimated contrast region labeling. ....	15
Figure 3.7	A-law based tone mapping example. The applied A is 5.97. ....	16
Figure 3.8	Diverse types of low-contrast image; (a) Low-intensity, low-contrast image; (b) High-intensity, low-contrast image; (c) Middle-intensity, low-contrast image. The red arrow represents the direction in which the enhancement stretches. ....	17
Figure 3.9	Two type of applied A-law function. (a) Typical A-law based tone mapping. (b) Modified A-law based tone mapping. ....	18
Figure 4.1	Experimental results of the proposed algorithm on the House image. (a) An input low contrast image, (b) contrast region labeling, the enhanced images (c) without and (d) with the weighting scheme for A-law based tone mapping, and (e) the changed probability distributions and the (f) changed cumulative distributions without (up) and with (below) the weighting scheme. ....	22

Figure 4.2	Experimental results of the proposed algorithm on the Dog image. (a) An input low contrast image, (b) contrast region labeling, the enhanced images (c) without and (d) with the weighting scheme for A-law based tone mapping, and (e) the changed probability distributions and the (f) changed cumulative distributions without (up) and with (below) the weighting scheme. ....	23
Figure 4.3	Experimental results of the proposed algorithm on the Village image. (a) An input low contrast image, (b) contrast region labeling, the enhanced images (c) without and (d) with the weighting scheme for A-law based tone mapping, and (e) the changed probability distributions and the (f) changed cumulative distributions without (up) and with (below) the weighting scheme.....	24
Figure 4.4	Experimental results of the proposed algorithm on the Baby image. (a) An input low contrast image, (b) contrast region labeling, the enhanced images (c) without and (d) with the weighting scheme for A-law based tone mapping, and (e) the changed probability distributions and the (f) changed cumulative distributions without (up) and with (below) the weighting scheme. ....	25
Figure 4.5	Experimental results of the proposed algorithm on the Diver image. (a) An input low contrast image, (b) contrast region labeling, the enhanced images (c) without and (d) with the weighting scheme for A-law based tone mapping, and (e) the changed probability distributions and the (f) changed cumulative distributions without (up) and with (below) the weighting scheme. ....	26
Figure 4.6	Experimental results of the proposed algorithm on the Foggy image. (a) An input low contrast image, (b) contrast region labeling, the enhanced images (c) without and (d) with the weighting scheme for A-law based tone mapping, and (e) the changed probability distributions and the (f) changed cumulative distributions without (up) and with (below) the weighting scheme. ....	27
Figure 4.7	Experimental results of the proposed algorithm on the Airplane image. (a) An input low contrast image, (b) contrast region labeling, the enhanced images (c) without and (d) with the weighting scheme for A-law based tone mapping, and (e) the changed probability distributions and the (f) changed cumulative distributions without (up) and with (below) the weighting scheme. ....	28
Figure 4.8	Comparison of enhancement results on the House image. (a) An input low contrast image. The enhanced images by using (b) the proposed algorithm, (c) Shen et al.'s algorithm, and (d) Shuhang et al.'s algorithm, respectively. ....	29
Figure 4.9	Comparison of enhancement results on the Dog image. (a) An input low contrast image. The enhanced images by using (b) the proposed algorithm, (c) Shen et al.'s algorithm, and (d) Shuhang et al.'s algorithm, respectively. ....	29

Figure 4.10	Comparison of enhancement results on the Village image. (a) An input low contrast image. The enhanced images by using (b) the proposed algorithm, (c) Shen et al.'s algorithm, and (d) Shuhang et al.'s algorithm, respectively. ....	30
Figure 4.11	Comparison of enhancement results on the Baby image. (a) An input low contrast image. The enhanced images by using (b) the proposed algorithm, (c) Shen et al.'s algorithm, and (d) Shuhang et al.'s algorithm, respectively. ....	30
Figure 4.12	Comparison of enhancement results on the Diver image. (a) An input low contrast image. The enhanced images by using (b) the proposed algorithm, (c) Shen et al.'s algorithm, and (d) Shuhang et al.'s algorithm, respectively. ....	31
Figure 4.13	Comparison of enhancement results on the Foggy image. (a) An input low contrast image. The enhanced images by using (b) the proposed algorithm, (c) Shen et al.'s algorithm, and (d) Shuhang et al.'s algorithm, respectively. ....	31
Figure 4.14	Comparison of enhancement results on the Airplane image. (a) An input low contrast image. The enhanced images by using (b) the proposed algorithm, (c) Shen et al.'s algorithm, and (d) Shuhang et al.'s algorithm, respectively.. ....	32

## **Nomenclature**

**RGB** Red, Green, and Blue

# Chapter I

## Introduction

Image enhancement is a traditional research issue of image processing. The goal of image enhancement is to improve the quality of input low quality images, such as low-contrast images, hazy images and foggy images. Retinex theory, which was proposed by Land [1], has been used in many different ways for image enhancement. In Retinex theory, the observed image intensity is assumed to be a product of the image's reflectance and illumination. Jobson proposed single-scale Retinex (SSR) [2], where the illumination of an input image is estimated by the Gaussian-filtered color channel images. However, color-constancy preserving problem is not the only issue resulted from the enhancement of images; halo artifacts also occurs on the edges of objects as a result of Gaussian filtering.

To reduce these artifacts in SSR algorithm, modified Retinex algorithms were proposed including multi-scale Retinex (MSR) [3] and multi-scale Retinex color restoration (MSRCR) [4] by Jobson. Kimmel [5] solved the color-constancy preserving problem by using the HSV color space. This method enhanced the V channel and preserved the H and S channels. Elad [6] applied a bilateral filter to preserve the image's edges rather than using a Gaussian filter to estimate the illumination of the image. Meylan [7] applied a principle component analysis to an input RGB color space, then estimated the luminance of the image by taking the first principle component and determined the chrominance domains using the second and third principle components, respectively. Then the luminance component alone was processed for enhancement. Shen and Hwang [8] also used the HSV color space to address the color inconsistency problem, and they developed a smoothing filter by optimizing a cost function to reduce halo artifact. Ahn [9] applied a guided filter to preserve the image's edges, then estimated the illumination of the image and used the Y channel of the Yuv color space to solve the color inconsistency problem.

These Retinex-based algorithms were used to solve the conventional problems and to improve the quality of input images effectively; however, sometimes the improved results were unnatural. To address this, Shen et al. [8] and Shuhang et al. [12] divided the reflectance and estimated illumination of an image using each of the proposed filters for obtaining reasonable reflectance, the boundaries of which were 0 (Absolute Absorption) and 1 (Absolute Reflectance). Shen et al. [8] used gamma correction to obtain a natural image. Shuhang et al. [12] used a bi-log function as a method for cumulative distribution matching in order to enhance the image more naturally.

In this thesis, the term *low-contrast image* is defined. As shown in the blue circle of Figure 1.1(c),

the probability distribution of an image intensity is concentrated within a certain region. These distributions decrease the visibility of the image, as shown in Figure 1.1(a). Thus, the purpose of enhancement in the present study was to increase the visibility of an image by stretching the probability distribution of a low-contrast image. In this work, the low-contrast image is enhanced using the proposed adaptive bilateral filter to solve the halo artifact problem on the object's edges. This process allows the estimated reflectance to have the range from 0 to 1. The estimated illumination is enhanced using the proposed adaptive A-law based tone mapping for improving the low-contrast regions naturally. By improving the image's probability distribution using adaptive bilateral filtering and A-Law based tone mapping, an enhanced image is obtained as shown in Figure 1.1(b), which exhibits also more uniform distribution of intensity values as shown in Figure 1.1(d).

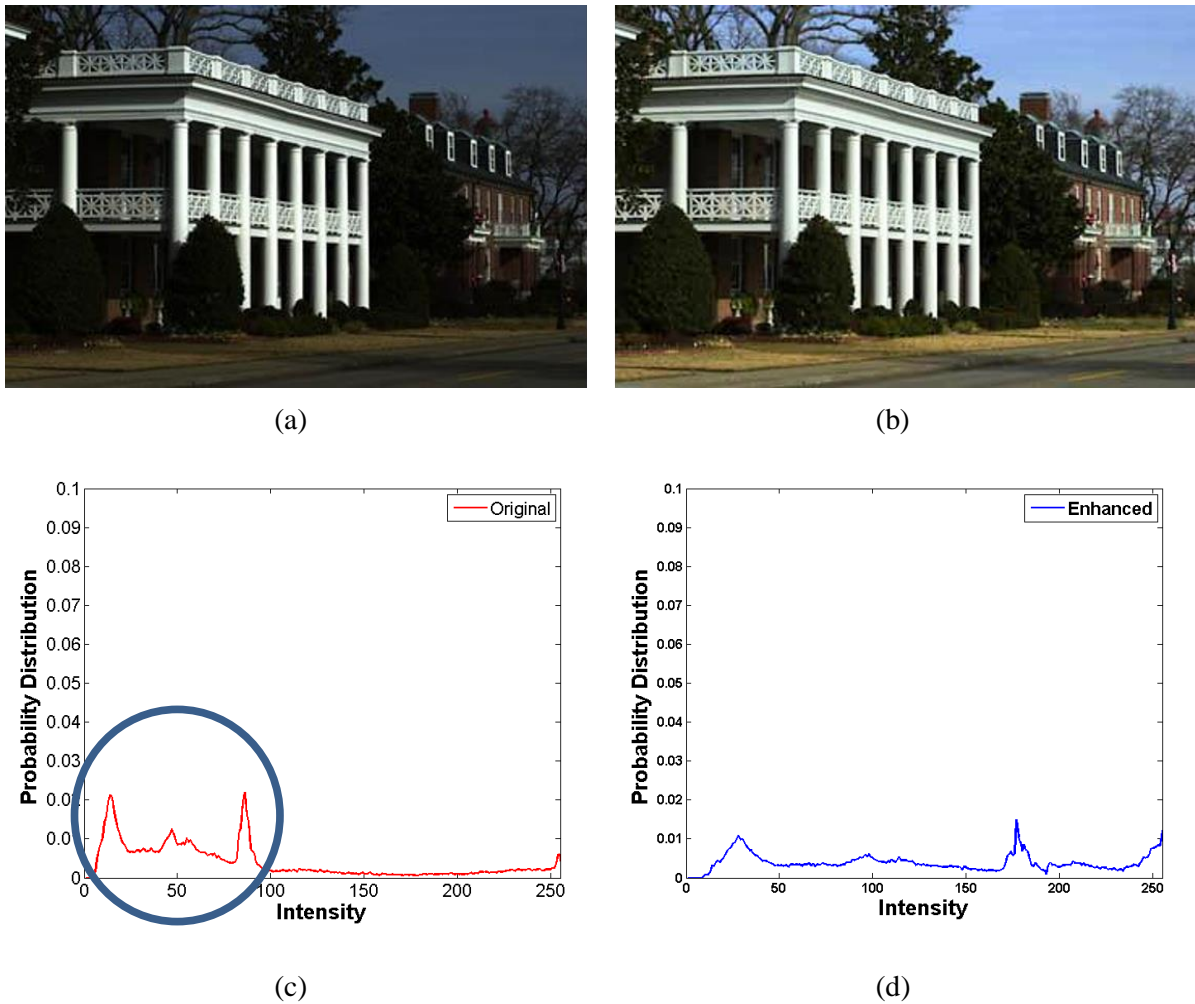


Figure 1.1: Low contrast image enhancement. (a) An input low contrast image and (b) the enhanced image. Probability distributions of (c) input Y channel and (d) the enhanced Y channel.

Our algorithm can be described as follows. First, we estimate the illumination of the Y channel

instead of the RGB color space using an adaptive bilateral filter. This process also allows us to separate the reflectance from the low-contrast image. Second, we estimate the low, middle, and high contrast regions, which are defined according to a cost function, which is based on the density of estimated illumination. Third, we apply the adaptive A-law based tone mapping using the estimated contrast regions, respectively. Finally, we obtain the enhanced image by transforming the Y channel—which is a product of the enhanced illumination and separated reflectance—and the original u and v channels into the RGB color space.

This thesis is organized as follows. Chapter 2 presents the related work. Chapter 3 describes the proposed algorithm for enhancing the low-contrast image. Chapter 4 shows the experimental results. Chapter 5 includes the conclusion.

## Chapter II

### Previous Works

#### 2.1 Retinex based on RGB Color Space

In Retinex theory [1], image intensity  $I$  is represented by the product of image reflectance  $R$  and illumination  $L$  given by

$$I(x, y) = R(x, y) \cdot L(x, y). \quad (2.1)$$

In the SSR algorithm [2], the Gaussian filter convolution, along with the input image, estimates the illumination of the image. The result of SSR in  $i$  channel ( $i \in \{R, G, B\}$ ) is  $R_{S_i}(x, y)$ . Reflectance in the log scale is obtained by

$$R_{S_i}(x, y) = \log I_i(x, y) - \log[F(x, y) * I_i(x, y)], \quad (2.2)$$

where  $F(x, y)$  is a normalized Gaussian function [2], represented by

$$F(x, y) = K \cdot \exp\left(-\frac{x^2+y^2}{c^2}\right), \quad (2.3)$$

where  $c$  is the Gaussian constant as scale,  $K$  is a normalization parameter. These are used to satisfy  $\sum_x \sum_y F(x, y) = 1$ . However, the SSR algorithm has a halo artifact problem on the edges of objects and a color-constancy problem caused by color shifting.

Figure 2.1 shows the SSR results and the problems created by the SSR algorithm. Figure 2.1 (a) and (b) show a low-contrast image and an SSR-result image, respectively. Figure 2.1 (c) and (d) show enlarged images of a blue rectangle from Figure 2.1 (a) and (b), respectively. As shown in Figure 2.1 (d), the overall color of SSR result becomes reddish. This indicates that color constancy is not preserved as a result of the SSR algorithm. Figure 2.1 (e) shows an enlarged image of the red rectangle from Figure 2.1 (b). This image shows the halo artifact problem occurring on the edges of objects.

To reduce halo artifact caused by the Gaussian constant  $c$  of the SSR algorithm, the MSR algorithm was proposed by Jobson [3]. A result of MSR,  $R_{M_i}(x, y)$  is yielded by the weighted sum of  $R_{S_i}(x, y)$  at multiple image scales.



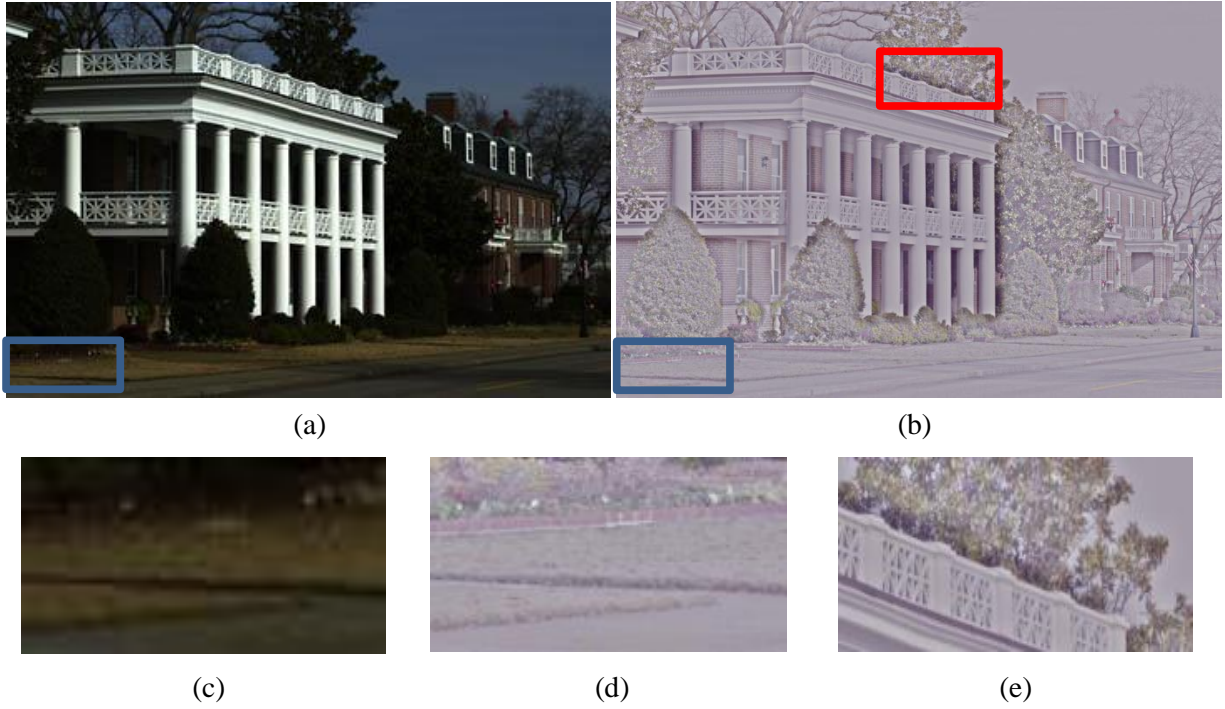


Figure 2.1: Retinex-based image enhancement. (a) An input low contrast image and (b) the enhanced image by using SSR. The enlarged images of the blue rectangles in (c) the input image and (d) the enhanced image. (e) The enlarged image of the red rectangle in the enhanced image.

$$R_{M_i}(x, y) = \sum_{n=1}^N w_n \cdot R_{S_i, n}(x, y), \quad (2.4)$$

where  $N$  is the number of scales and  $w_n$  is the following weighting parameter:  $\frac{1}{N}$ . Meanwhile,  $R_{S_i, n}$  is an SSR result of  $i$  channel in the  $n$ -th scale. As shown in Figure 2.2(a), the MSR algorithm solved the halo artifact problem. However, the overall image color does not appear to be natural. Thus, MSR cannot solve the color constancy problem. For this reason, MSRCR was proposed by Jobson [4] to solve the color constancy problem of the MSR algorithm. The result of MSRCR  $R_{M_{C_i}}(x, y)$  is yielded by the product of the color restoration function and the results of MSR.

$$R_{M_{C_i}}(x, y) = C_i(x, y) \cdot R_{M_i}(x, y), \quad (2.5)$$

where  $C_i(x, y)$  is the color restoration function.

$$C_i(x, y) = \beta \log[\alpha I'_i(x, y)], \quad I'_i(x, y) = \frac{I_i(x, y)}{\sum_{i=1}^S I_i(x, y)}, \quad (2.6)$$

where  $I'_i(x, y)$  is the ratio of  $i$  color channel to the whole channel and  $\alpha, \beta$  is constant.



(a)

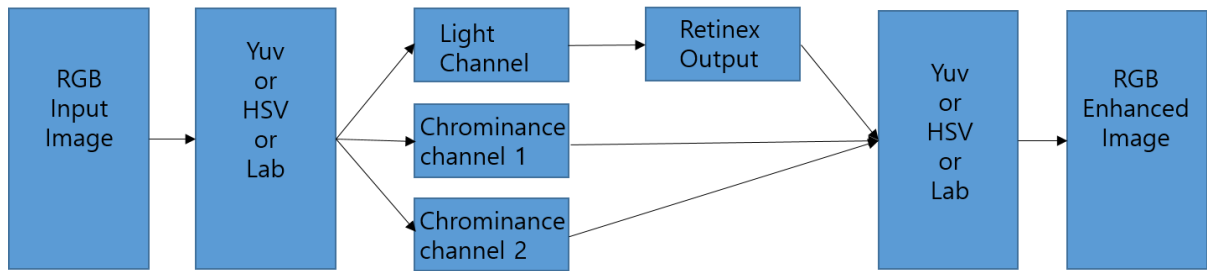
(b)

Figure 2.2: Comparison of image enhancement results: (a) MSR and (b) MSRCR.

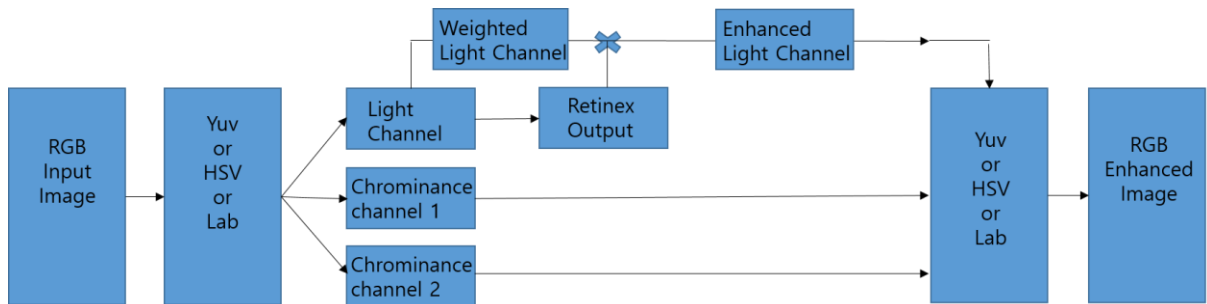
As shown in Figure 2.2(b), the MSRCR algorithm causes greater enhancement than MSR in terms of the color constancy problem; however, MSRCR cannot perfectly solve both the halo artifact and the color constancy problems.

## 2.2 Retinex based on Light Channel

To solve the color constancy problem, Retinex algorithms using light-channel were proposed by [5], [8], and [9]. These algorithms used the V channel of the HSV color space or the Y channel of the Yuv color space, which represent the light information. Figure 2.3 shows the flow charts and the results of these algorithms.



(a).



(b)



(c)



(d)

Figure 2.3: Light channel based Retinex algorithms. The flow charts of (a) [9] and (b) [8] and [9]. The enhanced images by using (c) [9] and (d) [8] and [9].

Figure 2.3(a) shows the Retinex algorithm flow chart using the light information channel. The RGB color channel is converted into light and into a chrominance channel. These algorithms only use the light channel to preserve the color constancy of the image. They then improve the light channel using equation (2.2), but the bilateral filter or guided filter is applied to prevent the occurrence of halo artifacts. Finally, these algorithms convert the enhanced light and original chrominance channel into an RGB color channel. Figure 2.3(c) shows the results of Figure 2.3(a). In Figure 2.3(c), the light channel Retinex looks flat. This is because the light channel Retinex loses the ordering of the light channel, though it still preserves the color constancy and enhances the detail of the image. Thus, these algorithms generally use light channels as weight factors for solving the problem of flat-looking images, as shown in Figure 2.3(b). Figure 2.3(d) shows how these algorithms solve the problem of flat-looking images.

## Chapter III

### Proposed Algorithm

#### 3.1 Overview

The typical Retinex-based image enhancement algorithms used a luminance channel, which is a channel that has been converted from an RGB color space, such as the Y channel of a Yuv color space or the V channel of an HSV color space. The algorithm developed in the present study also uses the Y channel of a Yuv color space to preserve the color constancy of the image. To estimate the illumination of the image, we apply an adaptive bilateral filter to the Y channel to estimate the illumination of the image. Then, we estimate the low-contrast region of the estimated illumination using cost function and cost labeling to enhance the adaptiveness of the image. We obtain enhanced illumination by applying adaptive A-law based tone mapping based on the low-contrast region that has been estimated during the previous processing. Finally, we yield the enhanced Y channel, which produces multiple of enhanced illumination and reflectance. Then, we obtain an enhanced RGB image, which has been converted from the enhanced Y channel and the original u and v channel.

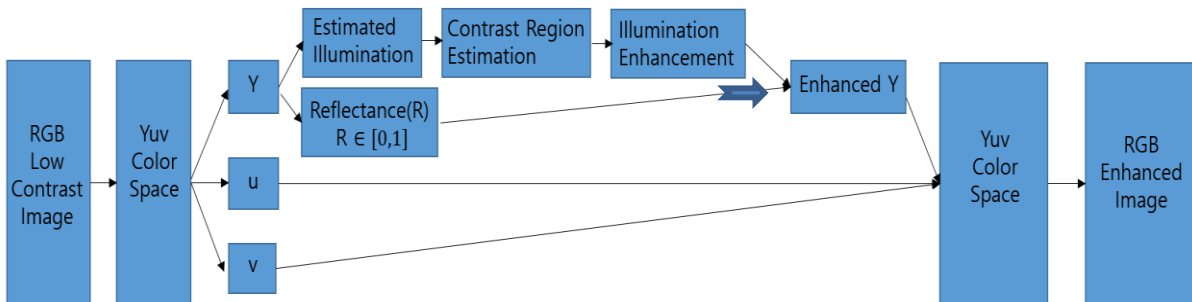


Figure 3.1: Flowchart of the proposed algorithm.

#### 3.2 Adaptive Bilateral Filtering

According to the Retinex theory [1], the observed intensity of the Y channel image is represented as the product of the related reflectance and illumination.

$$I_{lum}(x, y) = R_{lum}(x, y) \cdot L_{lum}(x, y) \quad (3.1)$$

where  $I_{lum}(x, y)$ ,  $R_{lum}(x, y)$ , and  $L_{lum}(x, y)$  reflect the intensity, reflectance, and illumination at the pixel position  $(x, y)$  in the Y channel image. Note that because the reflectance is normalized into  $[0,1]$ ,  $I_{lum}(x, y) \leq L_{lum}(x, y)$ .

The conventional Retinex-based algorithms estimate the illumination of an image by performing convolution on the input image using conventional smoothing filters, such as the Gaussian [2,3], bilateral [6], or guided filters [9]. The Gaussian filter computes the average pixel value of the neighboring pixel set, and thus it often causes halo artifacts. In contrast to this, the bilateral filter [10] and guided filter [11] can preserve the edges of an input image; thus, these filters can reduce the number of halo artifacts. Note that conventional bilateral filtering assigns a greater weight to neighboring pixels  $\mathbf{q}(u, v)$  that are closer to any given pixel  $\mathbf{p}(x, y)$  and that have more similar pixel values to  $\mathbf{p}(x, y)$ . However, in some pixels, the estimated illumination values can be smaller than the corresponding intensity values due to the smoothing nature of the used filters. This effect results in reflectance values larger than 1.

Therefore, we propose the use of the adaptive bilateral filter in our algorithm in order to obtain a reasonable range of reflectance. More specifically, at a given pixel  $\mathbf{p}(x, y)$ , we only consider the neighboring pixels  $\mathbf{q}(u, v)$  's with larger intensity values than those of  $\mathbf{p}(x, y)$  and similar colors to  $\mathbf{p}$ . So, let  $P(x, y)$  represent the set of neighboring pixels to  $\mathbf{p}(x, y)$ . We obtain the required set  $S(x, y)$  of pixels by sorting only the pixels from  $P(x, y)$ , which have larger intensity values than that of  $\mathbf{p}(x, y)$ , and which have similar colors to  $\mathbf{p}$ .

$$S(x, y) = \{(u, v) | (u, v) \in P(x, y), I_{lum}(u, v) > I_{lum}(x, y), d_{chr}(x, y, u, v) < \tau_{chr}\} \quad (3.2)$$

where the chrominance distance  $d_{chr}(x, y, u, v)$  between  $(x, y)$  and  $(u, v)$  is computed as

$$d_{chr}(x, y, u, v) = \sqrt{(I_u(x, y) - I_u(u, v))^2 + (I_v(x, y) - I_v(u, v))^2} \quad (3.3)$$

$I_u$  and  $I_v$  are u and v channel images in Yuv color space. and  $\tau_{chr}$  is given threshold which is empirically set as  $\tau_{chr} = 0.025$ .

Figure 3.2 shows the difference between the neighboring sets of the bilateral filtering and the adaptive bilateral filtering (ABF). The red rectangle in Figure 3.2(a) represents the set of neighboring pixels to  $\mathbf{p}(x, y)$  in the bilateral filtering, and the black rectangle in Figure 3.2(b) represents the set of neighboring pixels to  $\mathbf{p}(x, y)$  in the ABF. The blue and black check signs in Figure 3.2(b) represent the images with the larger intensity and similar color, respectively.

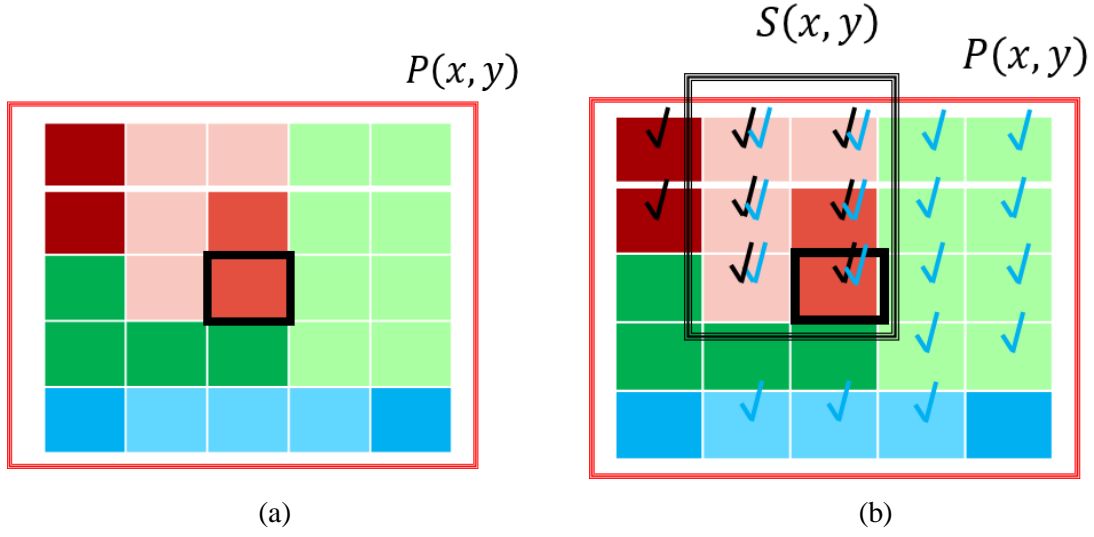


Figure 3.2: Neighboring pixels in ABF. (a) Neighboring set  $P(x, y)$  of  $(x, y)$  in bilateral filtering. (b) Neighboring set  $S(x, y)$  of  $(x, y)$  in ABF.

Then we estimate the illumination value at  $(x, y)$  as

$$\hat{L}_{lum}(x, y) = \frac{\sum_{(u,v) \in S(x,y)} F_{geo}(u, v) \cdot F_{int}(u, v) \cdot I_{lum}(u, v)}{\sum_{(u,v) \in S(x,y)} F_{geo}(u, v) \cdot F_{int}(u, v)} \quad (3.4)$$

where  $F_{geo}(u, v)$  and  $F_{int}(u, v)$  denote the geometric similarity and intensity similarity in bilateral filtering

$$F_{geo}(u, v) = \frac{1}{2\pi\sigma_1^2} \exp\left(-\frac{(x-u)^2 + (y-v)^2}{2\sigma_1^2}\right),$$

$$F_{int}(u, v) = \frac{1}{2\pi\sigma_2^2} \exp\left(-\frac{(I_{lum}(x,y) - I_{lum}(u,v))^2}{2\sigma_2^2}\right), \quad (3.5)$$

where we set  $\sigma_1 = 3$  and  $\sigma_2 = 5$ .

Note that the original bilateral filtering is implemented by replacing  $S(x, y)$  with  $P(x, y)$  in the above equation (3.4). Because we only consider the neighboring pixels, which have larger luminance values than  $\mathbf{p}(x, y)$ , we can guarantee that the resulting estimated illumination values lie within the available range of  $[0, 1]$  according to equation (3.1). Moreover, we can further enhance the details and preserve the edge structure of the inputted image by smoothing the neighboring pixels that have similar colors to the current pixel.

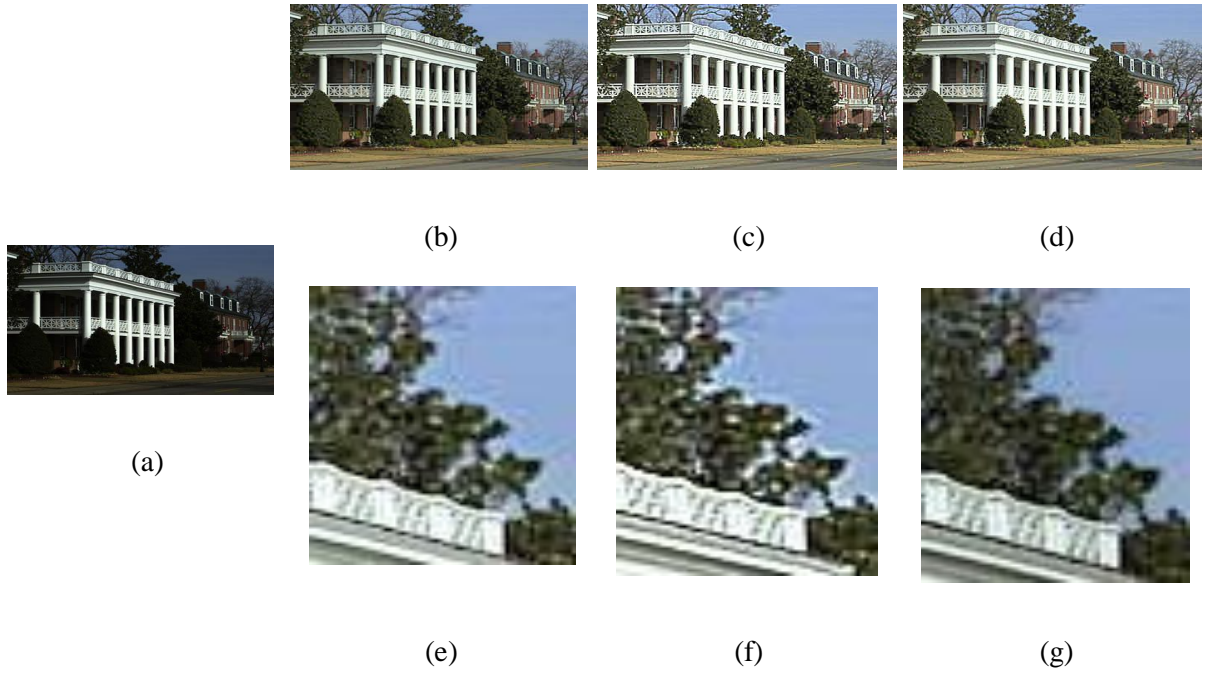


Figure 3.3: Results of ABF. (a) Original image. (b) Bilateral filtering result. (c) Guided filtering result. (d) ABF result. (e), (f), and (g) are the enlarged images of (b), (c), and (d), respectively.

Then, from equation (3.1), we obtain reflectance as

$$R_{lum}(x, y) = \frac{I_{lum}(x, y)}{\hat{L}_{lum}(x, y)}. \quad (3.6)$$

We enhance the low-contrast input image by improving the range of the estimated illumination image's  $\hat{L}_{lum}$ 's intensity.

Figure 3.3 shows the result of the ABF, as well as those of other edge-preserving filters. Using three filters to enhance low-contrast images is an effective method of enhancement. However, the results of the bilateral filtering and guided filtering have some halo artifacts, as shown in Figure 3.3(e) and (f). On the other hand, the result of the ABF not only solves the halo artifact problem, but also maintains the naturalness of the image.

### 3.3 Contrast Region Partitioning

We define the low-contrast region, middle-contrast region, and high-contrast region according to the degree of density in each given histogram region. More specifically, if the given histogram region is dense, normal, or diffused, then we define that region as low-contrast, middle-contrast, and high-contrast, respectively.



For low-contrast image enhancement, the low-contrast region is stretched, the high-contrast region is compressed, and the middle-contrast region is maintained. Thus, we must determine which regions are low-contrast, middle-contrast, and high-contrast in order to enhance the low-contrast image.

### 3.3.1 Global Estimation

We divide the histogram, which represents the probability density of the estimated illumination of the image  $\hat{L}_{lum}$ , into 16 regions in order to determine the contrast region. We then calculate the average value of the histogram in each region. We evaluate this value using cost-function  $C_i$  and determine the label of contrast region  $D_i$ , as shown in Figure 3.4(a).

$$C_i = \text{sign}(avp_i - \tau_c) \cdot \exp(|1000 \cdot (avp_i - \tau_c)|) \quad (3.7)$$

where  $avp_i$  is the average value of the histogram in  $i$ -th region,  $\tau_c = 0.006$ ,

$$D_i = \begin{cases} L & \text{if } C_i \geq 0, \\ M & \text{if } -10 \leq C_i < 0, \\ H & \text{Otherwise.} \end{cases} \quad (3.8)$$

The cost function and standard of labeling are set empirically. If two adjacent regions have the same label  $D_i$ , the two regions merge together. From this process, the global low-contrast region is determined, as shown in Figure 3.4(b). L, M, and H of Figure 3.4 represent the low-contrast region, middle-contrast region, and high-contrast region, respectively.

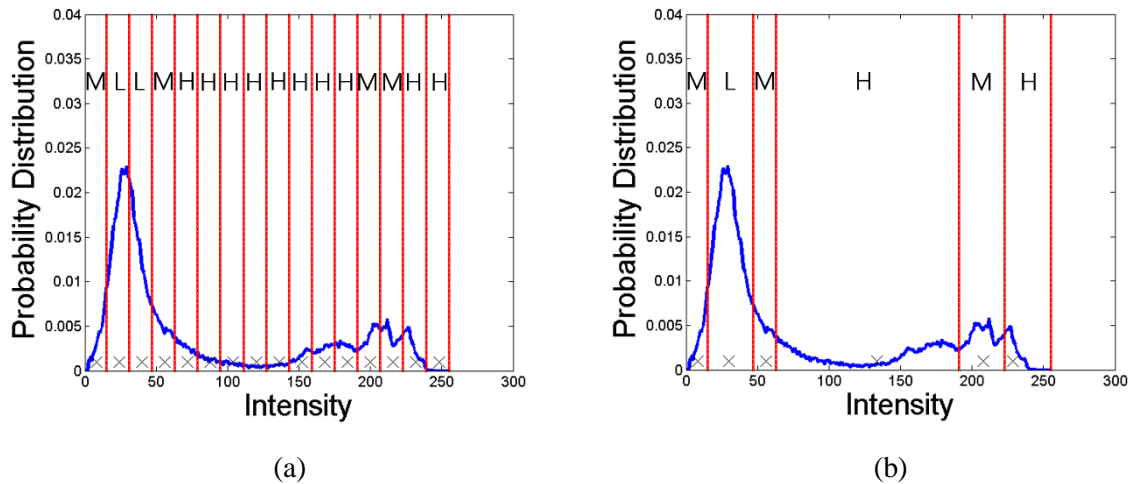


Figure 3.4: Global estimation for low contrast region. (a) Initial contrast region labeling. (b) Merged contrast region labeling.

### 3.3.2 Local Estimation

Both sides of a determined region cannot satisfy the condition of the included region. Therefore, the side region of merged regions is checked by using equations (3.7) and (3.8), then determines whether extension or compression has occurred. More specifically, when the low-contrast image's histogram and the merged estimated contrast region are labeled, as in Figure 3.5 (a), the left side of the low-contrast region is not evaluated precisely. To address this, we check the local contrast region (the red and black rectangles), which has been placed in the start or end region (indicated by the yellow line) of the low-contrast region, whether this region is low-contrast or not. If the labeling of the checked region is not the same as the original labeling, the checked region changes its labeling, and the labeling of the start or end region also changes. From these process, we estimate the low-contrast region, as shown in Figure 3.5(b). This process occurs again in the middle-contrast region. The local estimation for the low-contrast region is then obtained, as shown in Figure 3.6(a).

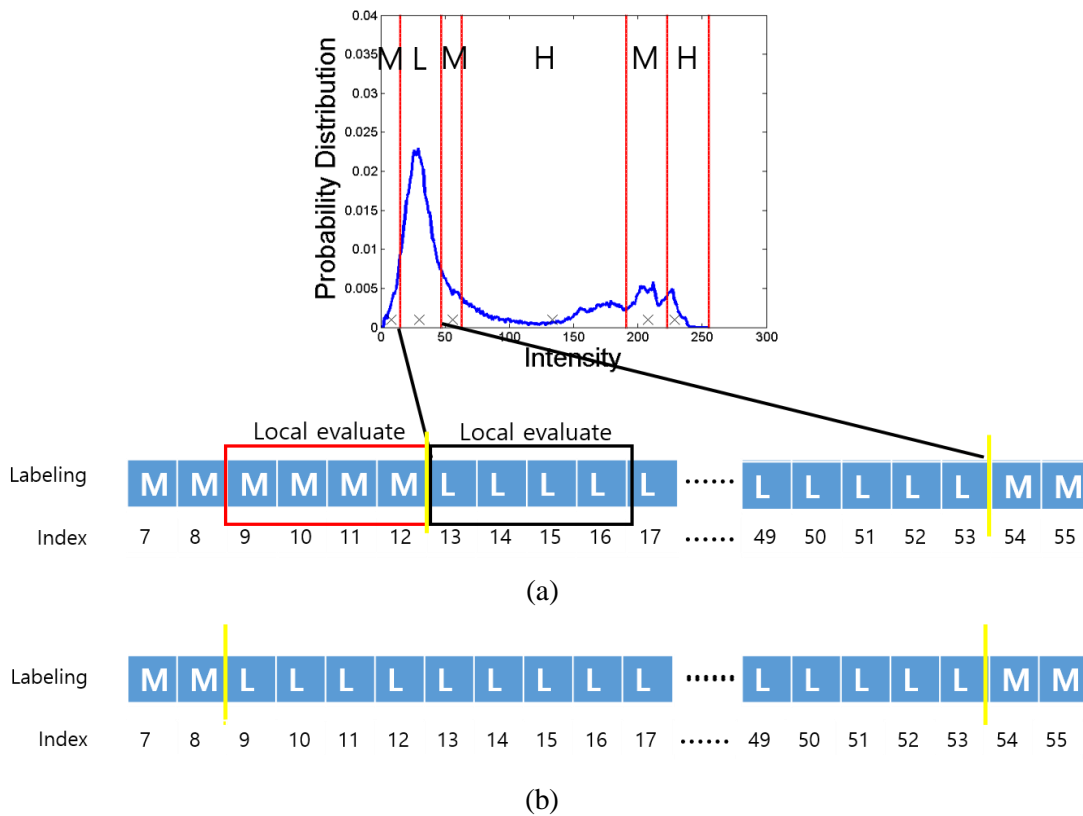


Figure 3.5: Local estimation for low-contrast region. (a) Process of local estimation. (b) Result of local estimation labeling.

### 3.3.3 Exception Handling

If the high-contrast regions are placed in low (0–30) or high (225–255) intensity, these regions will be absorbed into the adjacent regions. This not only causes less enhancement, but also reduces the quality of the visibility of the final output. Figure 3.6(b) shows the high-contrast region being absorbed into the adjacent middle-contrast region.

Additionally, if a high-contrast region, which has small range of about 20, is placed in a middle intensity region or middle-contrast region, which has a small range of about 20, is placed between regions that share the same labeling, then this region will be absorbed into an adjacent region for the same reason.

### 3.4 Adaptive A-law Based Tone-Mapping

Conventional histogram equalization or cumulative density function (CDF) matching can be used to enhance low-contrast images. However, the result of these methods are often unnatural, as intensity values that begin as being similar may be changed to become greatly different from one another.

Tone-mapping is a common technique used in image processing. This technique is used to map one set of an intensity domain to another set of the intensity domain as a given tone curve. If the tone curve is changed smoothly, the original similar intensity values may be maintained, and a similar intensity level may remain after tone-mapping. Thus, in the present study, we employ a tone-mapping curve to create a smooth change.

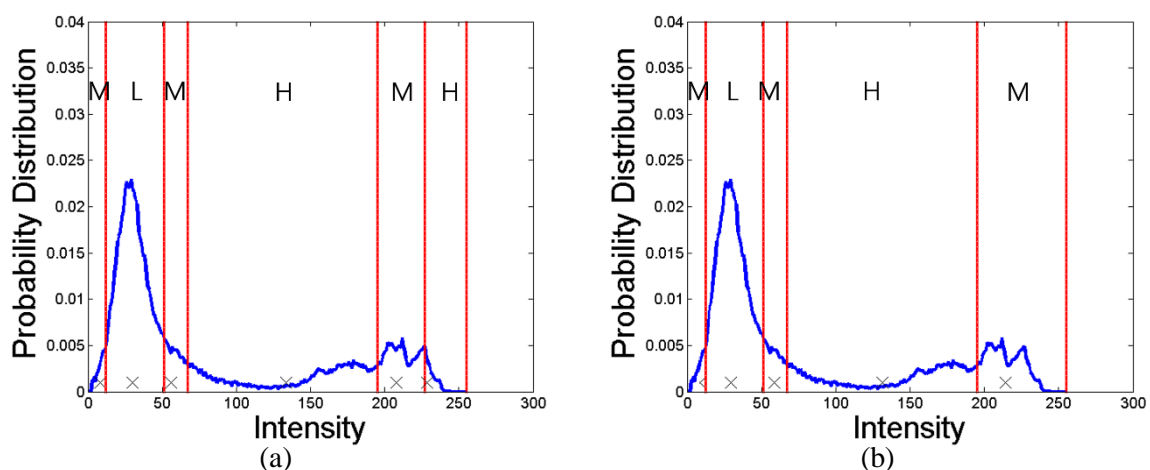


Figure 3.6: Exception handling of contrast region labeling. (a) Local contrast region labeling. (b) Final estimated contrast region labeling.

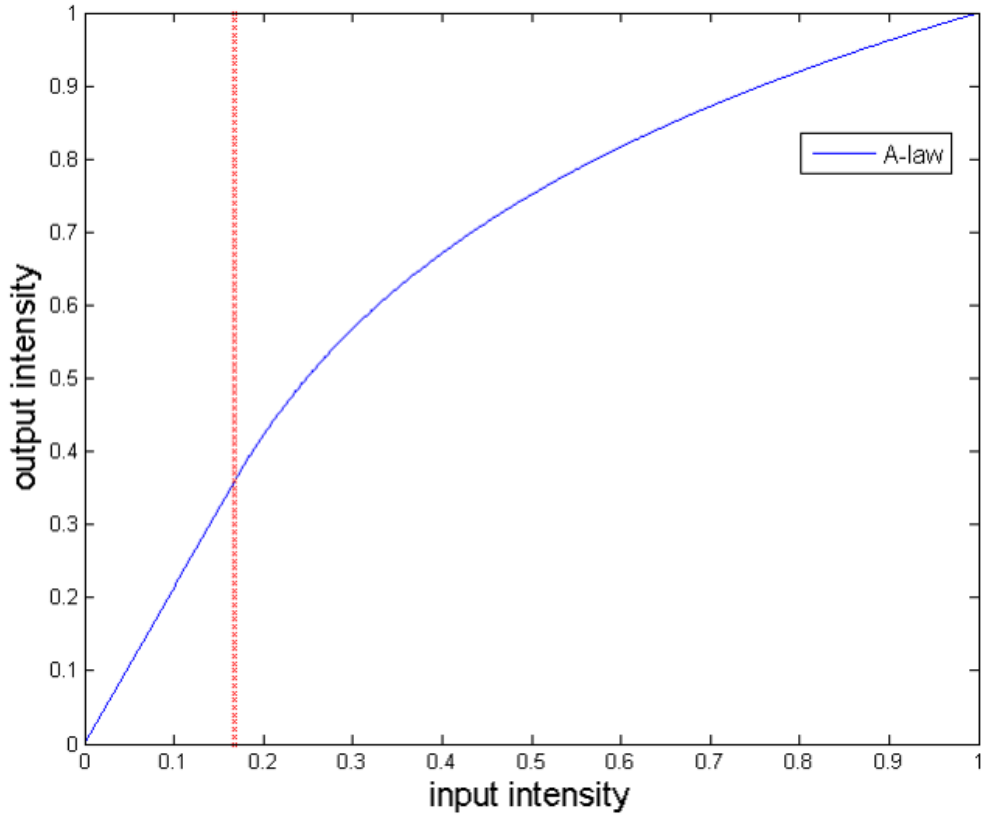


Figure 3.7: A-law based tone mapping example. The applied A value is 5.97.

### 3.4.1 A-law Based Tone Mapping

For low-contrast enhancement, we apply A-law based tone mapping. The A-law function is defined as

$$f_{A\text{-Law}}(z) = \begin{cases} \frac{A \cdot z}{1 + \log(A)} & \text{if } 0 \leq z \leq \frac{1}{A}, \\ \frac{1 + \log(A \cdot z)}{1 + \log(A)} & \text{if } \frac{1}{A} \leq z \leq 1, \end{cases} \quad (3.9)$$

where A is the A value of A-law, and A is larger than 1.

We analyze the straight line in Figure 3.7 (that is, the left part of the red line). In doing this, we are able to stretch the dense region, while the curved part of the line (the right part of the red line) can compress the diffused region. Thus, the use of A-law based tone mapping can improve the quality of low-contrast images.

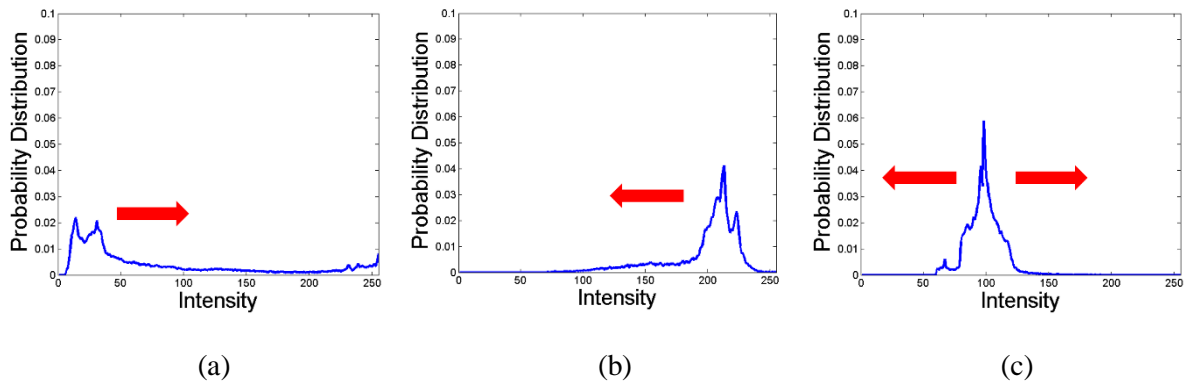


Figure 3.8: Diverse types of low-contrast image; (a) Low-intensity, low-contrast image; (b) High-intensity, low-contrast image; (c) Middle-intensity, low-contrast image. The red arrow represents the direction in which the enhancement stretches.

The enhancement of a low-contrast image stretches the dense region of the probability distribution. For example, if the low-contrast region is placed in a low- (Figure 3.8(a)) or high-intensity (Figure 3.8(b)) region, then the low-contrast region stretches only in one direction (the direction of the red arrow in Figure 3.8(a) and (b)). In this case, only one A-law function is applied. Also, if a low-contrast region is placed in a middle-intensity region (Figure 3.8(c)), then the low-contrast region stretches on both sides from the centroid of the low-contrast region.

Our algorithm does not change shape of the middle-contrast region. The other word, intensity interval in middle-contrast region are maintained after adaptive tone mapping. For this reason, we apply two types of A-law function. The first type is typical A-law based tone mapping (Figure 3.9(a)). In this type, the high- contrast region is placed next to a low-contrast region. The second type is modified A-law based tone mapping (Figure 3.9(b)). In this type, the middle-contrast region is placed between the low and high contrast regions. In this case, the applied A-law based tone mapping is the same as the first type in the low and high contrast regions. However, the middle-contrast region's shape must be maintained. For this reason, the middle-contrast region's intensity must either stay the same or shift while still preserving the region's shape. The slope of the middle-contrast region is 1 in the modified A-law based tone mapping.

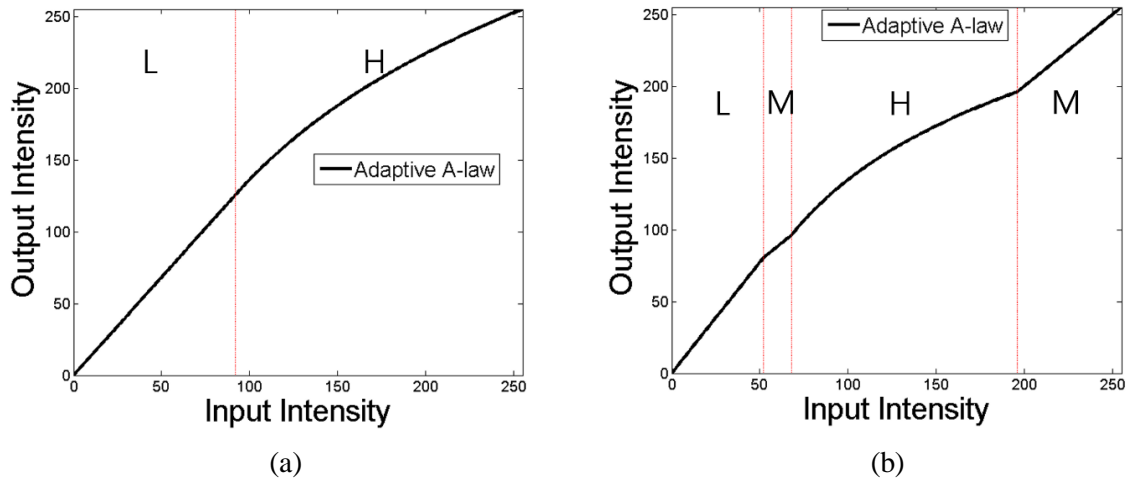


Figure 3.9: Two type of applied A-Law function. (a) Typical A-Law tone mapping. (b) Modified A-Law tone mapping.

The reciprocal of the A value is determined using the degree of straightness in the entire A-law function range, except for the middle-contrast region.

$$\frac{1}{A} = \frac{R(L_i)}{R(L_i) + R(H_i)} \tag{3.10}$$

where  $i$  is  $i$ -th A-law function,  $L_i$  and  $H_i$  are the low-contrast region and high-contrast region included in the  $i$ -th A-law function, and  $R(D_i)$  is the range of  $D_i$ .

### 3.4.2 Weighted A-law Based Tone Mapping

A value of the A-law function can determine the straight-line section, but it cannot control increasing quantity in intensity. This is because the A value determines not only the degree of the straight range, but also the increasing quantity of the A-law function. Additionally, if the A value is small, the other word ratio of the low-contrast region is quite high, then the increasing quantity in A-law based tone mapping is also small. In the same vein, if the middle-contrast region exists in a low-contrast image, this also causes a reduction of the slope in A-law based tone mapping.

So we apply the weight concept as:

$$f_{WA-Law}(z) = \begin{cases} \frac{W \cdot A \cdot z}{W + \log(A)} & \text{if } 0 \leq z \leq \frac{1}{A}, \\ \frac{W + \log(A \cdot z)}{W + \log(A)} & \text{if } \frac{1}{A} \leq z \leq 1, \end{cases} \quad (3.11)$$

where  $W$  is the weight value. It is determined as

$$W = \frac{\sum h(L_i)}{\sum h(H_i)} \log(A_i) \quad (3.12)$$

where  $h(D_i)$  is the histogram of probability density of  $D_i$ .

Using equations (3.11) and (3.12), we obtain the enhanced illumination of the low-contrast image  $\tilde{L}_{lum}$  as:

$$\tilde{L}_{lum}(x, y) = f_{WA-Law}(\hat{L}_{lum}(x, y)). \quad (3.13)$$

### 3. 5 Final Enhanced Image

From equation (3.13), we obtain the enhanced illumination  $\tilde{L}_{lum}$ . We already obtained the reflectance  $R_{lum}$  using ABF in Section 3.2 and equation (3.6). Therefore, the enhanced Y channel  $I_{enh}$  is obtained by  $\tilde{L}_{lum}$  and  $R_{lum}$  using equation (3.1), as follows:

$$I_{enh}(x, y) = R_{lum}(x, y) \cdot \tilde{L}_{lum}(x, y). \quad (3.14)$$

Finally, the image is obtained by converting the enhanced  $I_{enh}$  and original  $u$  and  $v$  to the enhanced RGB color space.

## Chapter IV

### Experimental Results

Our experiment used many low-contrast images to evaluate changes in probability distributions and cumulative distributions. Our algorithm was also compared to others, including those by Shen et al. [8] and Shuhang et al. [12]. All parameters used in our algorithm were determined experimentally and were fixed, such as  $\tau_{chr} = 0.025$  and  $\tau_c = 0.006$ .  $\sigma_1$  and  $\sigma_2$  had standard deviations of 3 and 5, respectively. Exception standards for estimating the low-contrast regions were also determined experimentally. The size of the adaptive bilateral filter window was  $11 \times 11$  for smoothing the neighbor pixels.

We applied A-law based tone mapping without and with weight in seven input images. The results of this application are shown in Figures 4.1–4.7. The low-contrast region of Figures 4.1(a), 4.2(a), 4.3(a), and 4.4(a) were placed in the low-intensity. Meanwhile, the low-contrast region of Figure 4.5(a), and 4.6(a) were placed in the middle-intensity and the low-contrast region of Figure 4.7(a) was placed in the high-intensity. Figures 4.1(c), 4.2(c), 4.3(c), and 4.4(c) show conventional A-law based tone mapping results. Figures 4.1(d), 4.2(d), 4.3(d), and 4.4(d) show weight A-law based tone mapping results. From these results, it can be concluded that weight A-law based tone mapping creates greater enhancement in images than conventional A-law based tone mapping in terms of visibility. Figures 4.1(e) and (f), 4.2(e) and (f), 4.3(e) and (f), and 4.4(e) and (f) show that weight A-law based tone mapping is more enhanceive than conventional A-law based tone mapping in terms of probability distribution and cumulative distribution. Figures 4.5(c), (d), (e), and (f); 4.6(c), (d), (e), and (f); and 4.7(c), (d), (e), and (f) show that conventional A-Law tone-mapping is better than weight A-law based tone mapping in terms of visibility, but that weight A-law based tone mapping is more enhanceive than conventional A-law based tone mapping in terms of probability distribution and cumulative distribution.

From the experimental results, we can see the importance of the low-contrast region's location. If the low-contrast region is placed in a low-intensity region, the use of weighted A-law based tone mapping is most appropriate, especially in terms of visibility, probability distribution, and cumulative distribution. If the low-contrast region is placed in a middle or high intensity region, then the use of A-law based tone mapping is more appropriate in terms of visibility, but the weighted A-law based tone mapping is better in terms of the other factors.

The results of comparison with this application and other algorithms are shown in Figures 4.8–4.14.

The method used by Shen et al. [8] is not ideal for enhancing all types of low-contrast image. As



shown in Figures 4.8(c), 4.9(c), 4.10(c), and 4.11(c), Shen et al.'s method [8] enhances low-intensity images; however, as shown in Figures 4.12(c), 4.13(c), and 4.14(c), this method is not appropriate for use with middle or high intensity, low-contrast image enhancement. Shen et al.'s algorithm [8] increases intensity to enhance low-contrast images, and this algorithm uses fixed tone-mapping despite the fact that the degree of darkness is different in every image. Thus, this method does not enhance all kinds of low-contrast images.

The method proposed by Shuhang et al. [12] efficiently enhances all types of low-contrast images while still preserving naturalness. Shuhang et al.'s algorithm [12] uses cumulative distribution matching to solve contrast problems. However, similar illumination values in the same low-contrast region can be changed too much by cumulative distribution matching. This causes distortion in the enhanced image. As shown in Figures 4.10(d), 4.11(d), 4.12(d), 4.13(d), and 4.14(d), Shuhang et al.'s method [12] preserves the original tone of the image and enhances it as well, but Figures 4.8(d) and 4.9(d) show that a distortion problem has occurred.

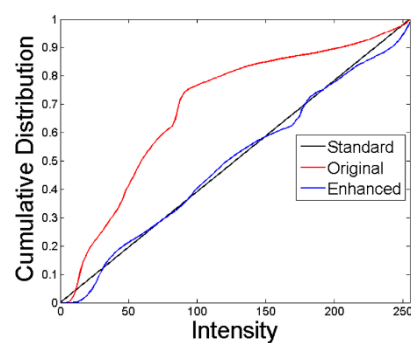
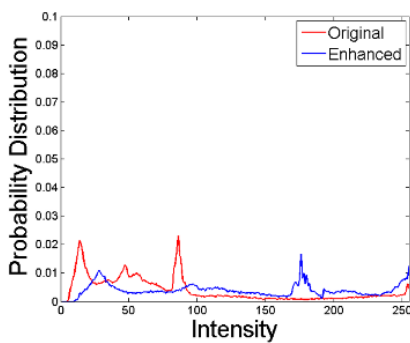
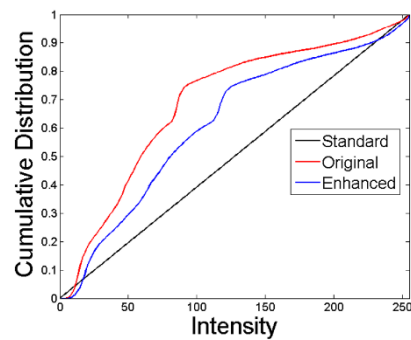
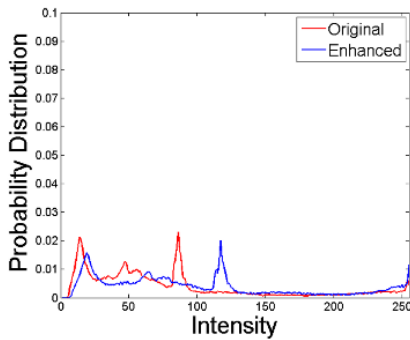
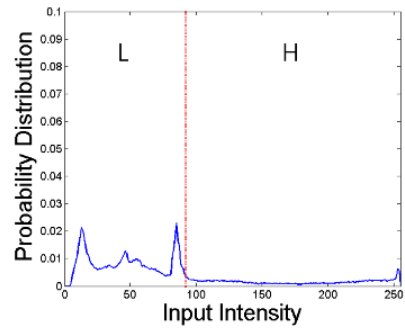


Figure 4.1: Experimental results of the proposed algorithm on the House image. (a) An input low contrast image, (b) contrast region labeling, the enhanced images (c) without and (d) with the weighting scheme for A-law based tone mapping, and (e) the changed probability distributions and the (f) changed cumulative distributions without (up) and with (below) the weighting scheme.

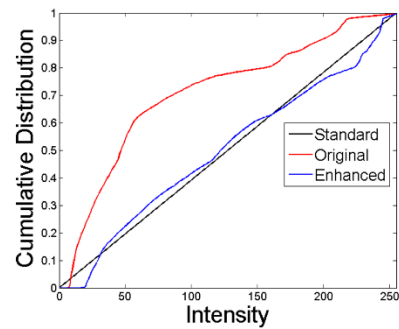
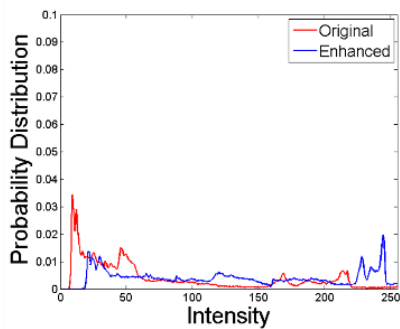
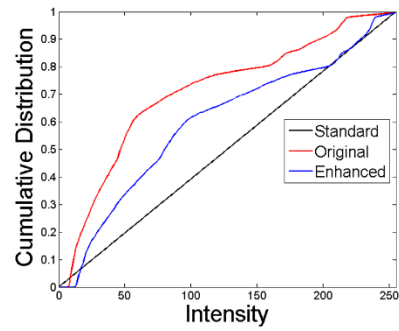
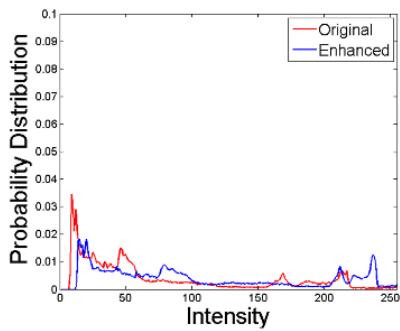
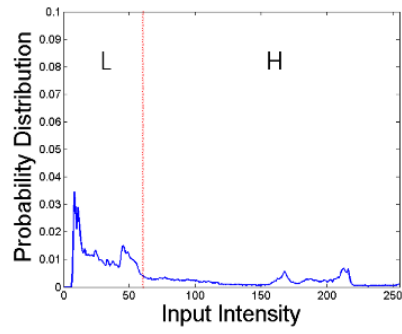
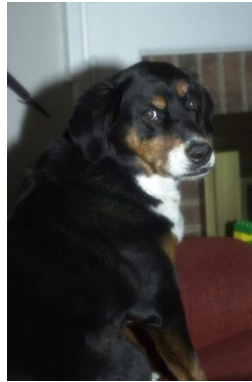


Figure 4.2: Experimental results of the proposed algorithm on the Dog image. (a) An input low contrast image, (b) contrast region labeling, the enhanced images (c) without and (d) with the weighting scheme for A-law based tone mapping, and (e) the changed probability distributions and the (f) changed cumulative distributions without (up) and with (below) the weighting scheme.

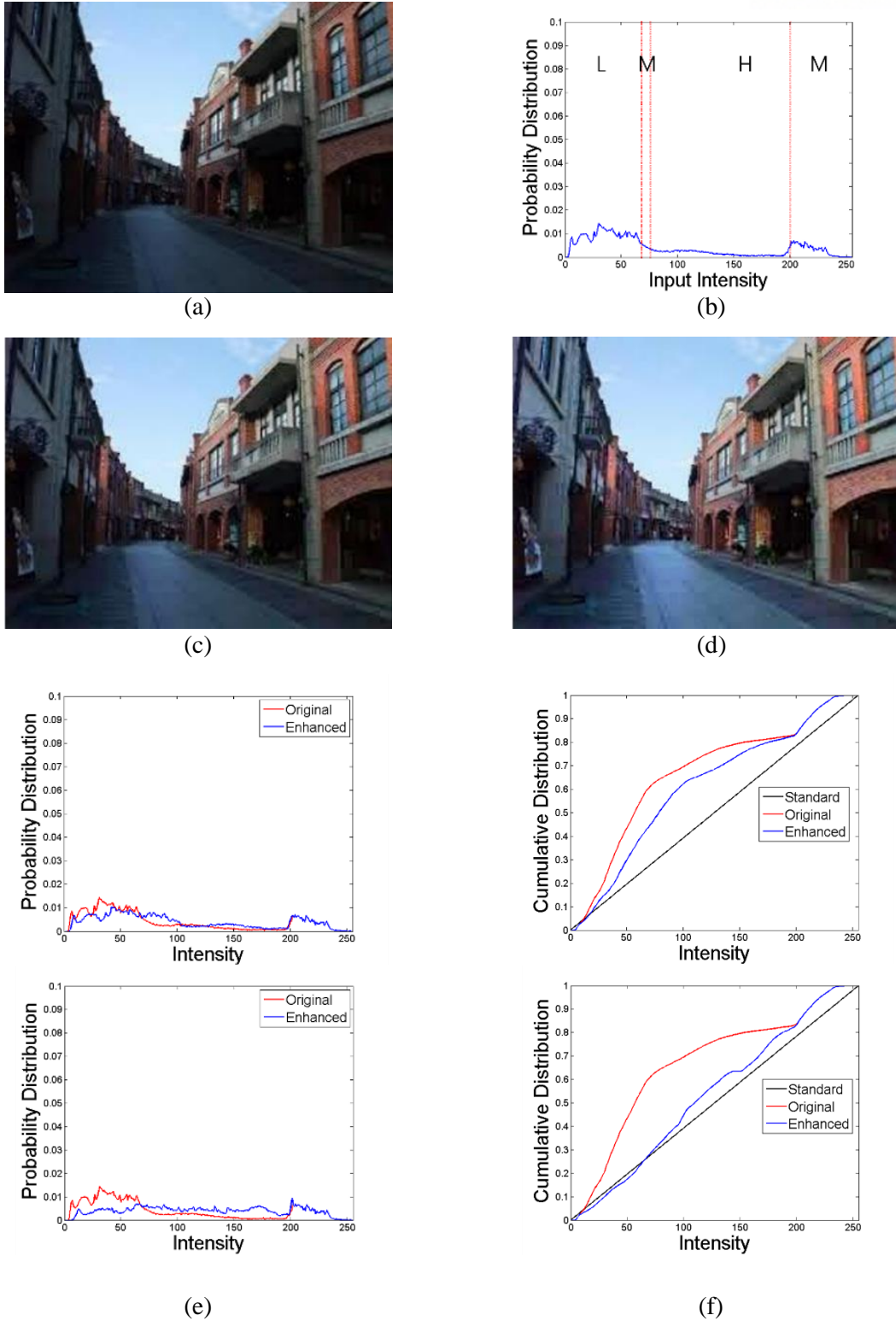


Figure 4.3: Experimental results of the proposed algorithm on the Village image. (a) An input low contrast image, (b) contrast region labeling, the enhanced images (c) without and (d) with the weighting scheme for A-law based tone mapping, and (e) the changed probability distributions and the (f) changed cumulative distributions without (up) and with (below) the weighting scheme.

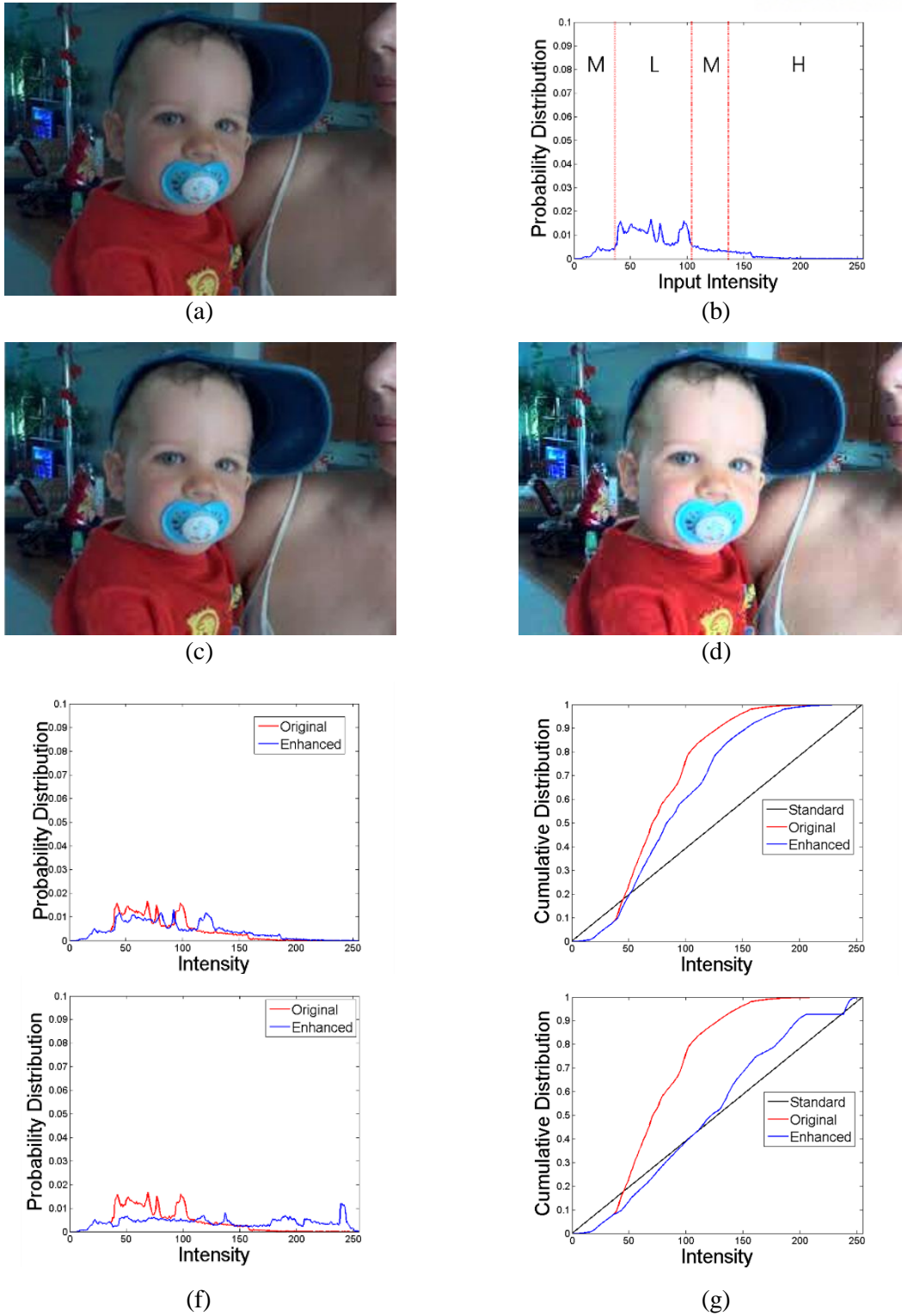


Figure 4.4: Experimental results of the proposed algorithm on the Baby image. (a) An input low contrast image, (b) contrast region labeling, the enhanced images (c) without and (d) with the weighting scheme for A-law based tone mapping, and (e) the changed probability distributions and the (f) changed cumulative distributions without (up) and with (below) the weighting scheme.

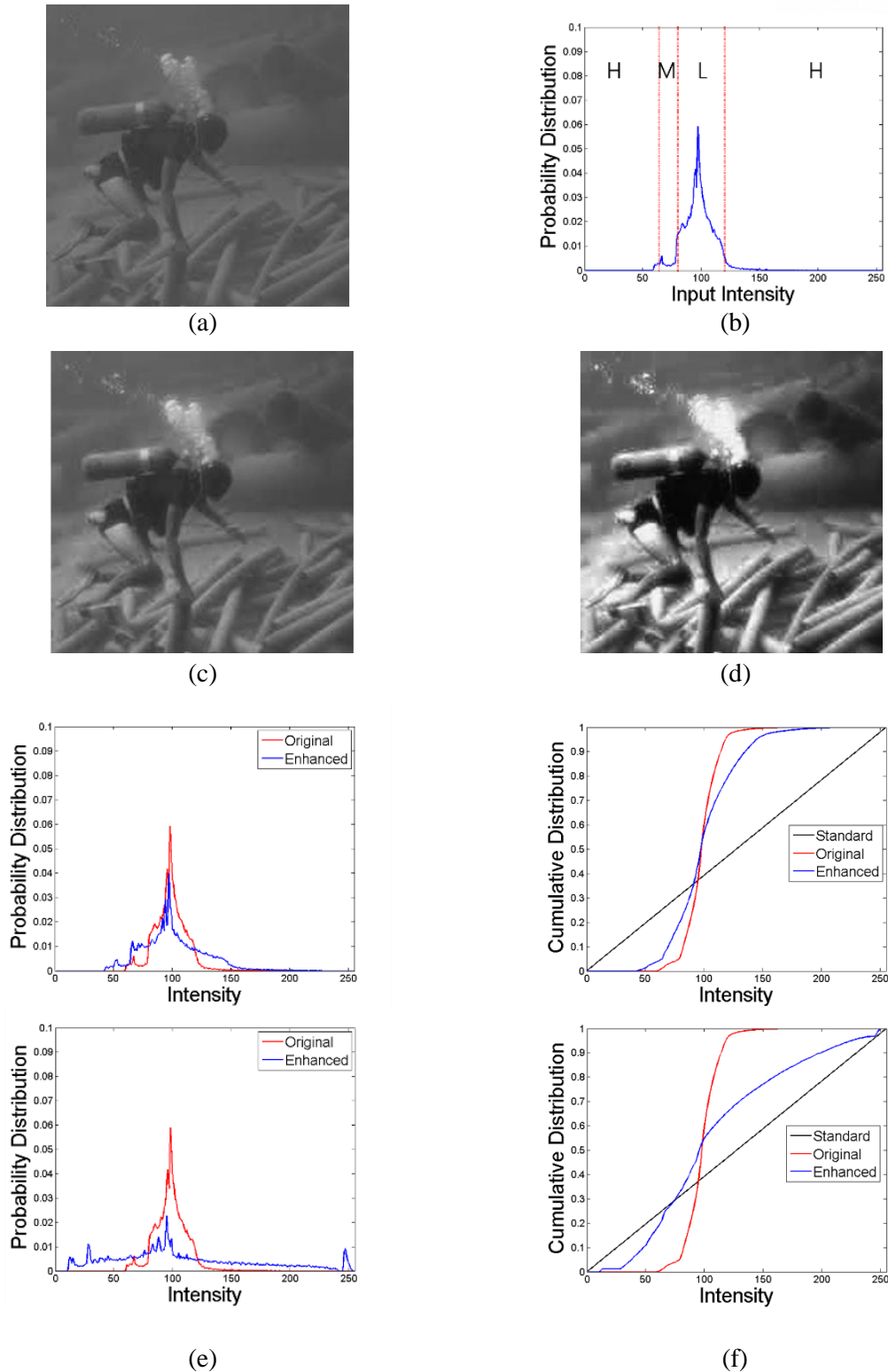


Figure 4.5: Experimental results of the proposed algorithm on the Diver image. (a) An input low contrast image, (b) contrast region labeling, the enhanced images (c) without and (d) with the weighting scheme for A-law based tone mapping, and (e) the changed probability distributions and the (f) changed cumulative distributions without (up) and with (below) the weighting scheme.

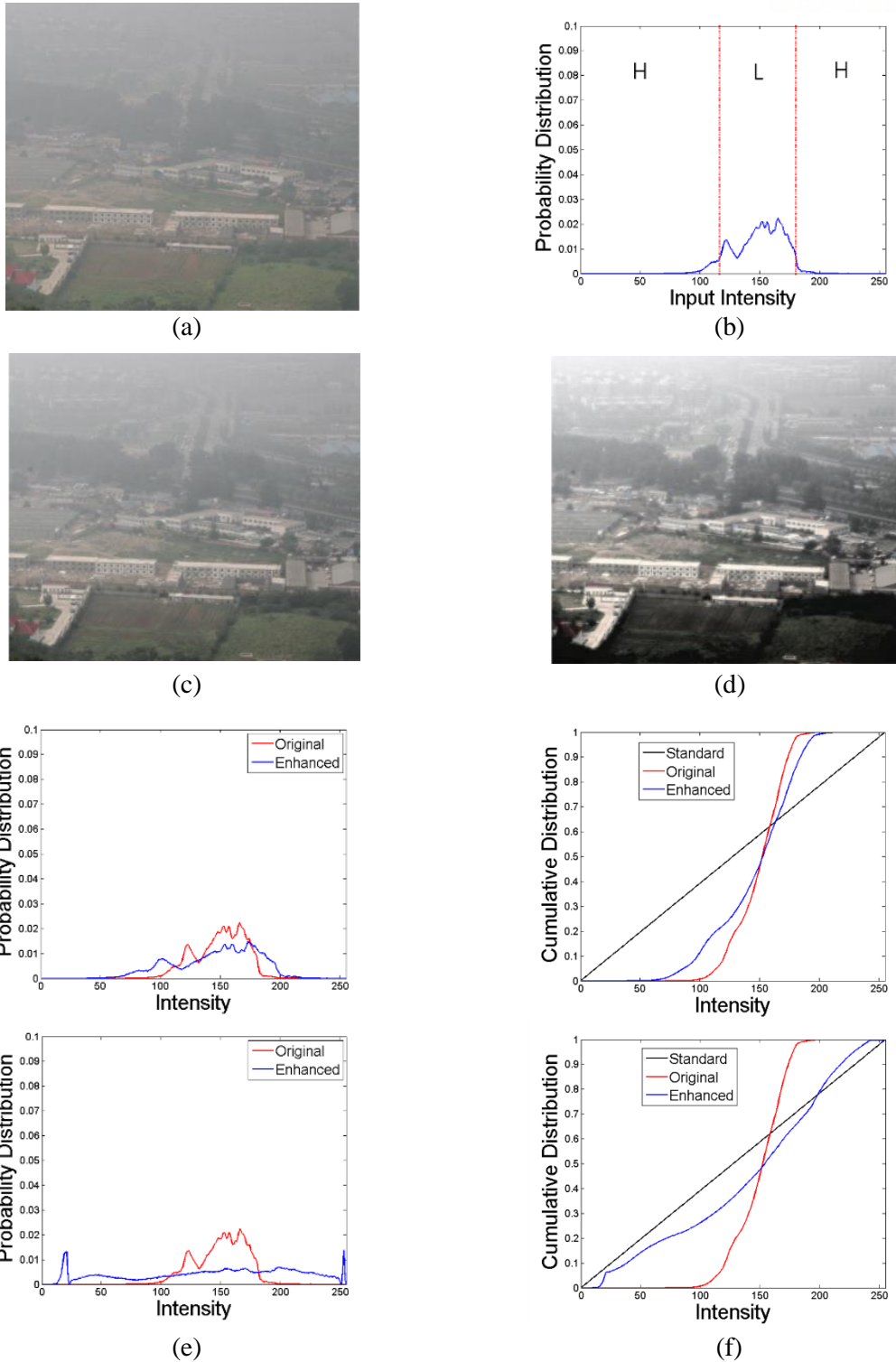


Figure 4.6: Experimental results of the proposed algorithm on the Foggy image. (a) An input low contrast image, (b) contrast region labeling, the enhanced images (c) without and (d) with the weighting scheme for A-law based tone mapping, and (e) the changed probability distributions and the (f) changed cumulative distributions without (up) and with (below) the weighting scheme.

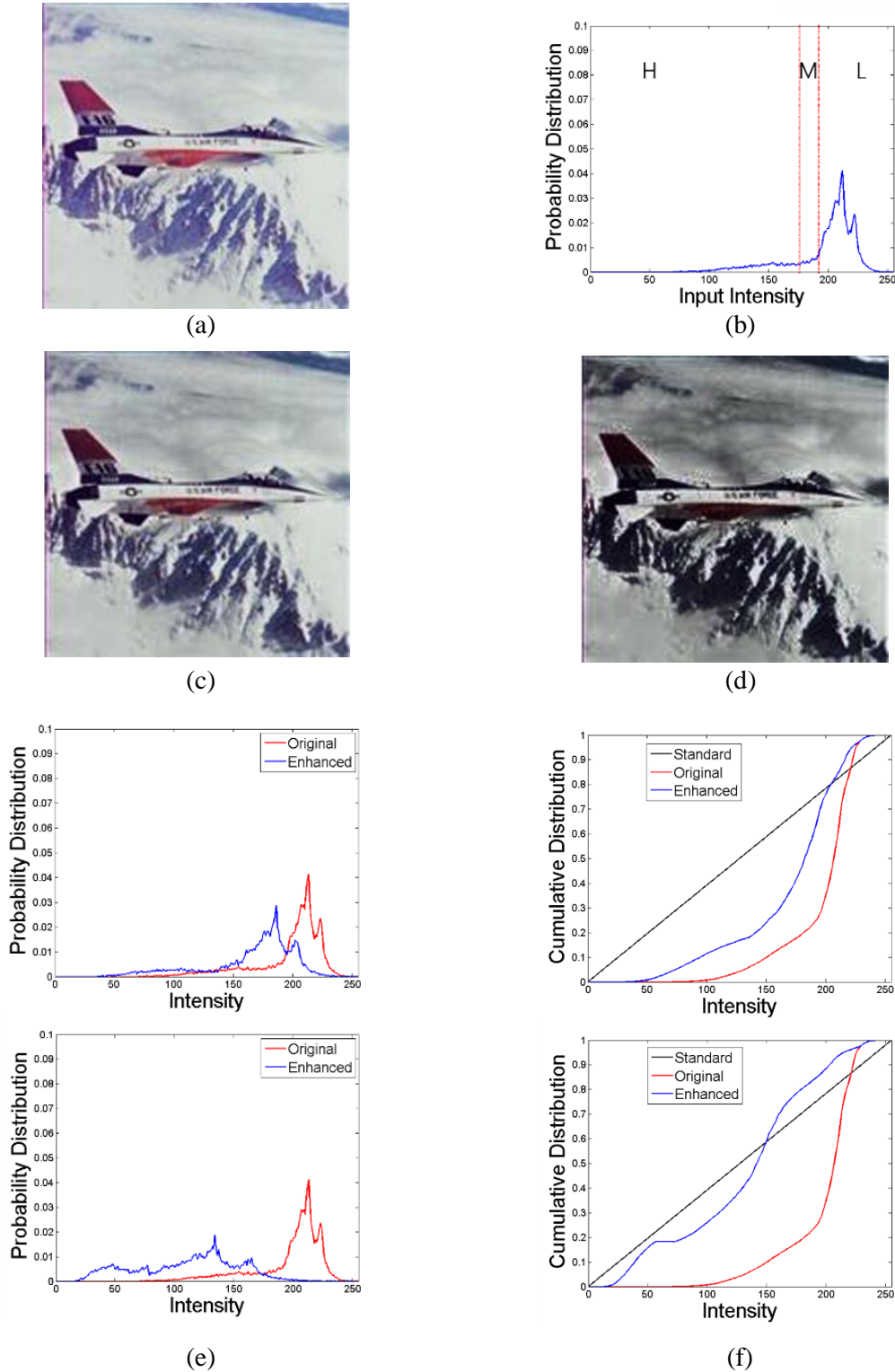


Figure 4.7: Experimental results of the proposed algorithm on the Airplane image. (a) An input low contrast image, (b) contrast region labeling, the enhanced images (c) without and (d) with the weighting scheme for A-law based tone mapping, and (e) the changed probability distributions and the (f) changed cumulative distributions without (up) and with (below) the weighting scheme.



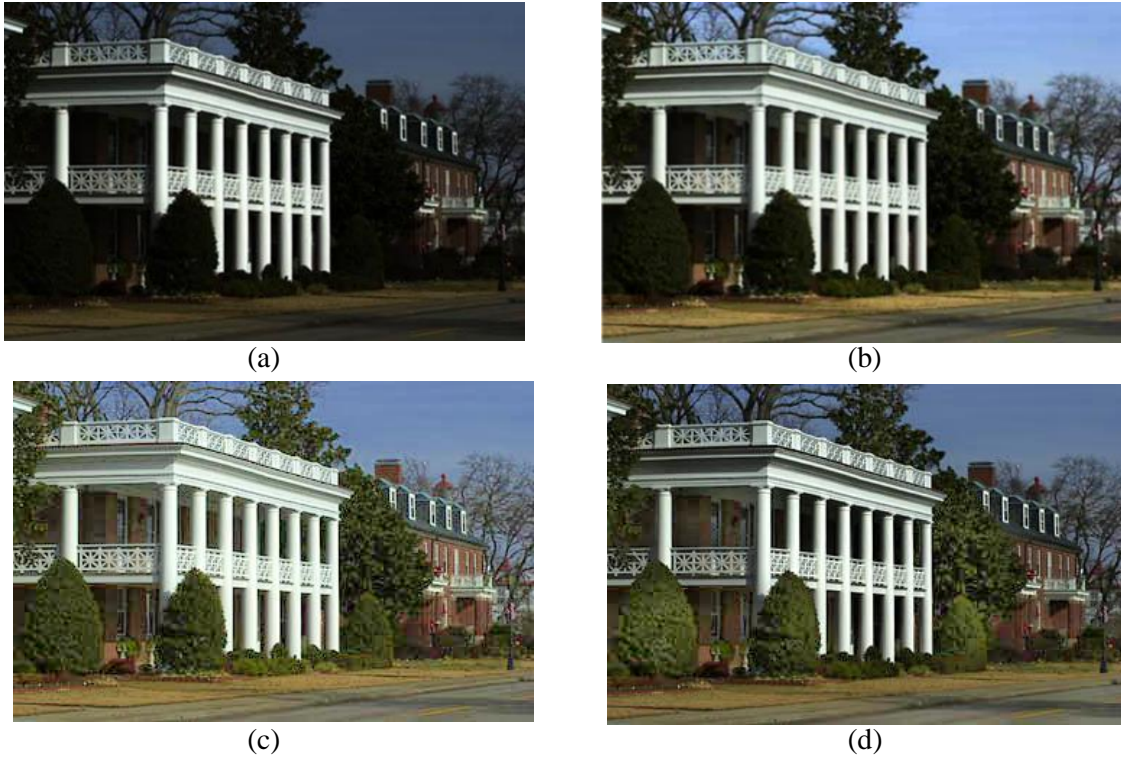


Figure 4.8: Comparison of enhancement results on the House image. (a) An input low contrast image. The enhanced images by using (b) the proposed algorithm, (c) Shen et al.'s algorithm, and (d) Shuhang et al.'s algorithm, respectively.

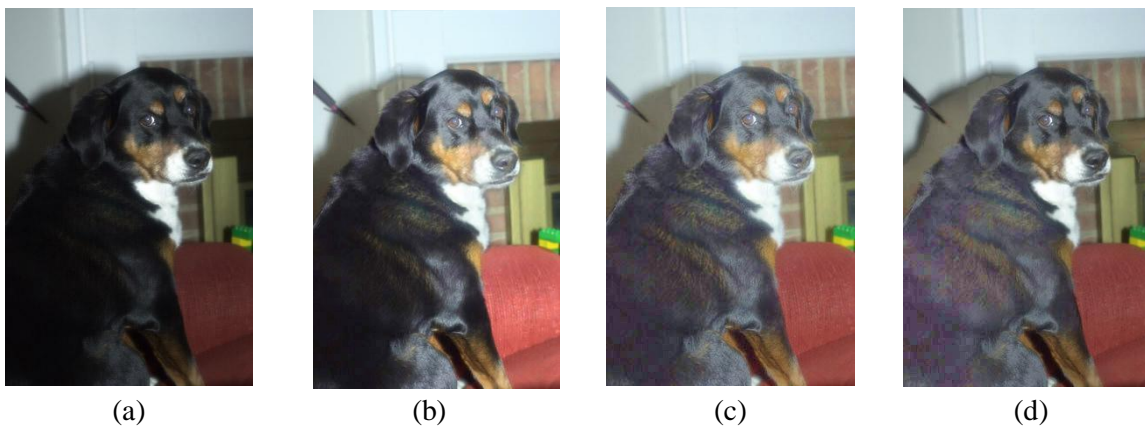


Figure 4.9: Comparison of enhancement results on the Dog image. (a) An input low contrast image. The enhanced images by using (b) the proposed algorithm, (c) Shen et al.'s algorithm, and (d) Shuhang et al.'s algorithm, respectively.



Figure 4.10: Comparison of enhancement results on the Village image. (a) An input low contrast image. The enhanced images by using (b) the proposed algorithm, (c) Shen et al.'s algorithm, and (d) Shuhang et al.'s algorithm, respectively.

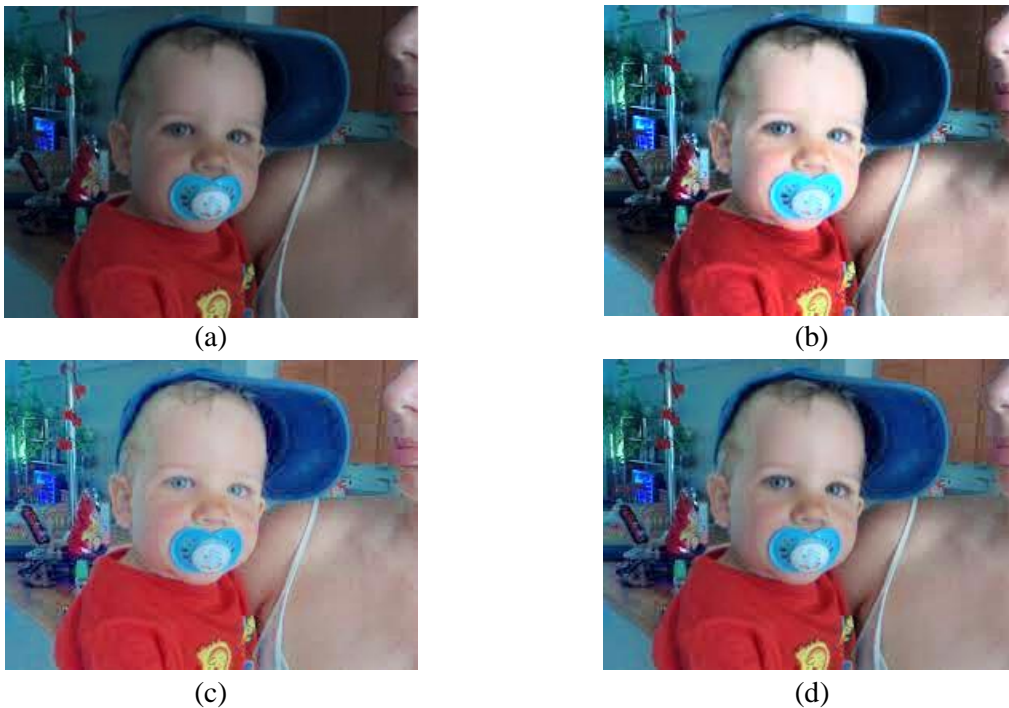


Figure 4.11: Comparison of enhancement results on the Baby image. (a) An input low contrast image. The enhanced images by using (b) the proposed algorithm, (c) Shen et al.'s algorithm, and (d) Shuhang et al.'s algorithm, respectively.

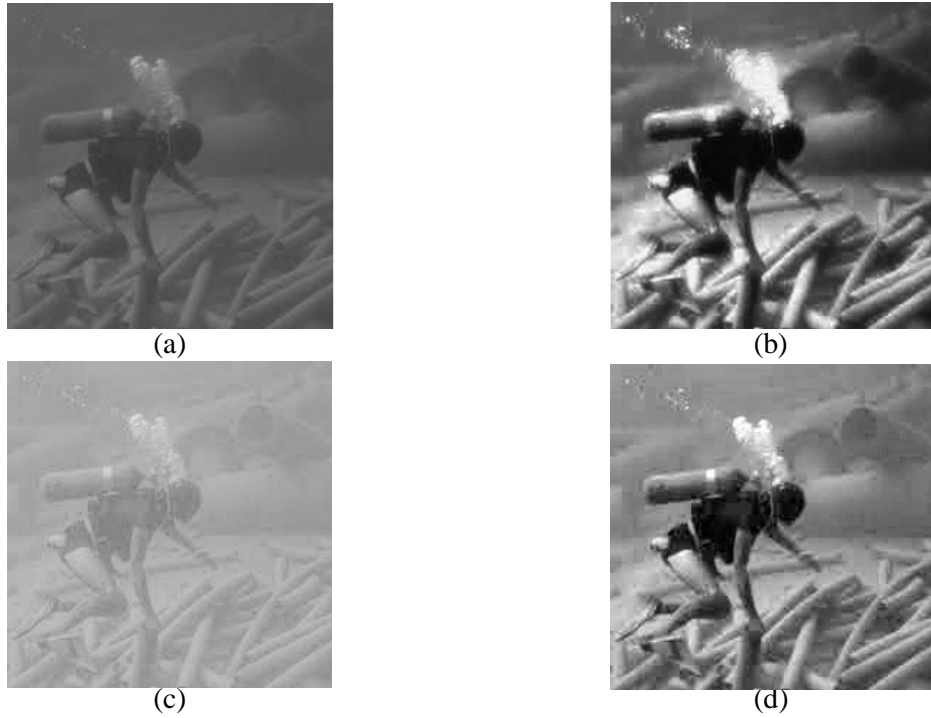


Figure 4.12: Comparison of enhancement results on the Diver image. (a) An input low contrast image. The enhanced images by using (b) the proposed algorithm, (c) Shen et al.'s algorithm, and (d) Shuhang et al.'s algorithm, respectively.

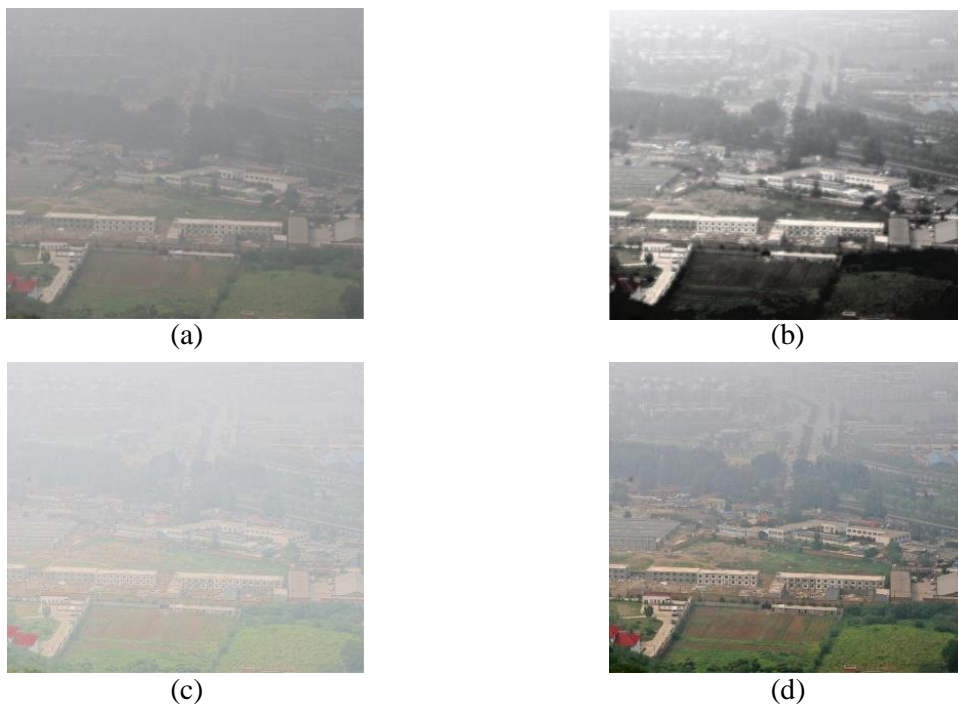


Figure 4.13: Comparison of enhancement results on the Foggy image. (a) An input low contrast image. The enhanced images by using (b) the proposed algorithm, (c) Shen et al.'s algorithm, and (d) Shuhang et al.'s algorithm, respectively.



(a)



(b)



(c)



(d)

Figure 4.14: Comparison of enhancement results on the Airplane image. (a) An input low contrast image. The enhanced images by using (b) the proposed algorithm, (c) Shen et al.'s algorithm, and (d) Shuhang et al.'s algorithm, respectively.

## Chapter V

### Conclusion

In this thesis, we proposed a low-contrast image enhancement algorithm using adaptive bilateral filtering and weighted A-Law tone-mapping. We solved halo artifact problem using adaptive bilateral filtering and preserved naturalness using adaptive A-law based tone mapping. Also, our algorithm solved a low-contrast image enhancement problem in terms of probability and cumulative distribution. The experimental results showed that the proposed algorithm enhances low contrast images efficiently.

## References

- [1] Land, Edwin H. *The retinex theory of color vision*, Scientific America., 1977.
- [2] Z.-u. Rahman, D. J. Jobson, and G. Woodell, "Multi-scale retinex for color image enhancement," in *Image Processing, IEEE International Conference on*, 1996, pp. 1003-1006.
- [3] D. J. Jobson, Z.-u. Rahman, and G. Woodell, "Properties and performance of a center/surround retinex," *Image Processing, IEEE Transactions on*, vol. 6, pp. 451-462, 1997.
- [4] D. J. Jobson, Z.-u. Rahman, and G. Woodell, "A multiscale retinex for bridging the gap between color images and the human observation of scenes," *Image Processing, IEEE Transactions on*, vol. 6, pp. 965-976, 1997.
- [5] R. Kimmel, M. Elad, D. Shaked, R. Keshet, and I. Sobel, "A variational framework for retinex," *International Journal of Computer Vision*, vol. 52, pp. 7-23, 2003.
- [6] M. Elad, "Retinex by two bilateral filters," in *Scale Space and PDE Methods in Computer Vision*, ed: Springer, 2005, pp. 217-229.
- [7] L. Meylan and S. Süsstrunk, "High dynamic range image rendering with a retinex-based adaptive filter," *Image Processing, IEEE Transactions on*, vol. 15, pp. 2820-2830, 2006.
- [8] C.-T. Shen and W.-L. Hwang, "Color image enhancement using retinex with robust envelope," in *Image Processing, International Conference on*, 2009, pp. 3141-3144.
- [9] H. Ahn, B. Keum, D. Kim, and H. S. Lee, "Adaptive local tone mapping based on retinex for high dynamic range images," in *Consumer Electronics, IEEE International Conference on*, 2013, pp. 153-156.
- [10] S. Paris, P. Kornprobst, J. Tumblin, and F. Durand, *Bilateral filtering: Theory and applications*: Now Publishers Inc, 2009.
- [11] K. He, J. Sun, and X. Tang, "Guided image filtering," *Pattern Analysis and Machine Intelligence, IEEE Transactions on*, vol. 35, pp. 1397-1409, 2013.
- [12] S. Wang, J. Zheng, H.-M. Hu, and B. Li, "Naturalness preserved enhancement algorithm for non-uniform illumination images," *Image Processing, IEEE Transactions on*, vol. 22, pp. 3538-3548, 2013.